geosciences

MDPI

Article

Evaluation of Jacking Forces in Weathered Phyllite Based on *In Situ* Pressuremeter Testing and Deep Learning

Lit Yen Yeo [1], Fredrik Phangkawira [2], Pei Gee Kueh [1], Sue Han Lee [1], Chung Siung Choo [1,*], Dongming Zhang [3,4] and Dominic Ek Leong Ong [5]

[1] Faculty of Engineering, Computing and Science, Swinburne University of Technology, Sarawak Campus, Kuching 93350, Sarawak, Malaysia; lyyeo@swinburne.edu.my (L.Y.Y.); 101214145@students.swinburne.edu.my (P.G.K.); shlee@swinburne.edu.my (S.H.L.)
[2] WSP Golder, Jakarta 12940, Indonesia; fredrik.phangkawira@wsp.com
[3] Key Laboratory of Geotechnical and Underground Engineering of Minister of Education, Tongji University, Shanghai 200092, China; 09zhang@tongji.edu.cn
[4] Department of Geotechnical Engineering, Tongji University, Shanghai 200092, China
[5] School of Engineering and Built Environment, Griffith University, Nathan Campus, Nathan, QLD 4111, Australia; d.ong@griffith.edu.au
* Correspondence: cschoo@swinburne.edu.my

Abstract: Pipe jacking is a trenchless technology used to install buried pipelines, such as sewer lines in wastewater management systems. Existing mechanistic approaches based on geomaterial strength parameters (i.e., friction angle and apparent cohesion) can provide an estimation of the potential jacking forces during construction. However, extracting intact rock cores for strength characterisation is challenging when dealing with highly weathered 'soft rocks' which exhibit RQD values of zero. Such was the case for a pipe jacking drive traversing the highly weathered lithology underlying Kuching City, Malaysia. Furthermore, mechanistic approaches face limitations during construction when jacking forces are dependent on operation parameters, such as jacking speed and lubrication. To address these knowledge gaps, the primary objectives of this study are the development of rock strength parameters based on *in situ* pressuremeter testing for the purpose of estimating jacking forces. Furthermore, this study investigates the influence of various pipe jacking operation parameters, with a particular focus on their impact on jacking forces in weathered 'soft rocks'. To achieve this, a novel deep learning model with an attention mechanism is introduced. The proposed methods of rock strength parameters derived from pressuremeter testing and the utilisation of deep learning will help to provide insights into the key factors affecting the development of jacking forces. This paper successfully shows the use of *in situ* pressuremeter testing in developing Mohr–Coulomb (MC) parameters directly from the site. In addition, the developed deep learning model with an attention mechanism successfully highlights the significance of pipe jacking operation parameters with an accuracy of 88% in predicting the jacking forces.

Keywords: pipe jacking; jacking forces; weathered phyllite; pressuremeter test; operation parameters; deep learning; attention mechanism

Citation: Yeo, L.Y.; Phangkawira, F.; Kueh, P.G.; Lee, S.H.; Choo, C.S.; Zhang, D.; Ong, D.E.L. Evaluation of Jacking Forces in Weathered Phyllite Based on *In Situ* Pressuremeter Testing and Deep Learning. *Geosciences* **2024**, *14*, 55. https://doi.org/10.3390/geosciences14030055

Academic Editors: Hongyuan Liu and Jesus Martinez-Frias

Received: 30 November 2023
Revised: 16 February 2024
Accepted: 17 February 2024
Published: 20 February 2024

1. Introduction

A unique challenge was faced in the construction of trunk sewer lines beneath the central business district (CBD) of Kuching. Under the Kuching Wastewater Management System project, 14.7 km of 1.5 m diameter trunk sewer lines were constructed via the pipe jacking method. These sewer lines were constructed to transport gravity-fed wastewater from over 7000 properties to a centralised wastewater treatment plant catering for 100,000 population equivalent (PE) [1]. The pipe jacking drives encountered highly weathered lithology [2], when the installation of these sewer pipelines reached depths of up to 35 m below the ground surface. At these depths, the trunk sewer lines were effectively

embedded within the weathered rocks underlying the Kuching CBD. The geology beneath Kuching city is relatively young and weathered Tuang formation which consists of highly fractured lithology such as sandstone, shale, phyllite and metagraywacke [2].

The highly weathered lithology caused difficulties in extracting sufficiently intact rock cores for rock strength testing. With adequate lengths of intact rock cores, it would be possible to conduct rock strength tests [3], such as the uniaxial compression strength test, triaxial test, point load test, shear wave velocity test or Brazilian tensile test [4–9]. However, the majority of recovered cores demonstrated rock quality designation (RQD) values of zero, where RQD is defined as the percentage of recovered cores exceeding 100 mm in length [10]. The phyllite underlying Kuching city has been reported to have characteristics of heavy weathering conditions with slickensides and steep dips [2]. The petrographic thin section analysis of phyllite in Kuching city showed compositions of mica, chlorite, grains of sericite, clay minerals, fine-grained quarts and carbonaceous materials, which have also been corroborated by the Geological Survey Department of Malaysia [2]. Some phyllite cores extracted from the project are shown in Figure 1, illustrating the lack of sufficient cores for rock strength testing.

Figure 1. Phyllite cores collected from soil investigation represent low RQD [11].

Rock strength parameters are necessary for computing frictional jacking forces. Many contemporary frictional jacking force models comprise closed-form mechanistic equations using rock strength parameters. These predictive frictional jacking force models are useful during the planning and design stages of pipe jacking construction. They rely on the geomaterial strength parameters, which are obtained from rock (or soil) strength tests performed on samples obtained from boreholes typically located at jacking shafts during the soil investigation phase. The accrued frictional resistance is dependent on lithology [11,12] as well as pipe jacking operation parameters [3,11,13–20].

Operation parameters can influence jacking forces, including jacking speed [15,17–19] and lubricant volume [11,13,14,21]. During construction, these operation parameters can deviate along the pipeline alignment. Additionally, borehole exploration is not commonly performed along the pipe alignment, leading to uncertainties in the geotechnical properties along the drive. Therefore, the precise impact of these operation parameters on jacking forces still needs to be better understood.

The current study aims to introduce methods for assessing the frictional jacking forces in highly weathered lithology. These methods will be demonstrated through a case study of a pipe jacking drive with a total drive distance of 120 m through highly weathered phyllite. *In situ* pressuremeter testing was used to develop rock strength parameters for the evaluation of jacking forces, which is fairly novel in direct measurements of weathered rock

masses from sites. The existing literature mainly focuses on laboratory conducted experiments such as using direct shear test for back analysis on jacking forces [3,11] and studying the arching phenomenon observed during pipe jacking [22]. Subsequently, deep learning techniques were applied to assess the influence of pipe jacking operation parameters on jacking forces through weathered rock, where most of the studies were performed to obtain higher prediction accuracy when predicting the complicated behaviour of underground soils and rocks [23]. The details of these techniques are described hereinafter.

2. Current Approaches for Assessing Frictional Jacking Forces

Existing predictive models of frictional jacking forces are based on Mohr–Coulomb (MC) strength parameters, i.e., apparent cohesion, C, and friction angle, ϕ. There have been previous attempts to develop MC strength parameters of rock masses, such as from direct measurements during drilling [24], and reconstitution of tunnelling rock spoil [11]. Table 1 shows some of these predictive models which incorporate soil arching effects. Soil arching reduces the normal stresses (and subsequently frictional forces) acting on the pipes. Some models considered the pipe–soil interface friction. However, it is important to note that the existing models are designed for drives encountered in soil conditions and could not be directly applied to pipe jacking drives traversing weathered rocks. Furthermore, these mechanistic models do not consider the influence of operation parameters towards frictional jacking forces. Table 2 shows the qualitative effects of different operation parameters on jacking forces.

Table 1. Mechanistic approach to predict the frictional jacking forces.

Reference	Jacking Force Model	Definition and Soil Strength Parameters		
[19]	$F = \mu_{int} \frac{\gamma r cos\left(45+\frac{\phi_r}{2}\right)}{tan\phi_r} \pi dl$	μ_{int}	=	pipe–soil interface frictional coefficient
		γ	=	unit weight of soil
		d	=	diameter of pipe
		r	=	radius of pipe
		l	=	length of pipe
		$\varnothing_r$	=	residual friction angle
[25]	$F = \beta(\pi D_e q + w) tan\frac{\phi'}{2} + \pi B_c C'$	C'	=	soil–pipe adhesion
		β	=	reduction factor of jacking force
		D_e	=	outer diameter of pipe
		q	=	normal force
		ϕ'	=	interface friction angle
		w	=	pipe weight
[17]	$F = \mu L D_e \frac{\pi}{2}\left[\left(\sigma_{EV} + \frac{\gamma D_e}{2}\right) + K_2\left(\sigma_{EV} + \frac{\gamma D_e}{2}\right)\right]$ $\sigma_{EV} = \frac{b\left(\gamma - \frac{2C}{b}\right)}{2K\tan\varnothing}\left(1 - e^{-2K\tan\varnothing\frac{h}{b}}\right)$ $b = D_e\left[1 + 2\tan\left(\frac{\pi}{4} - \frac{\varnothing}{2}\right)\right]$	C	=	soil cohesion
		$\varnothing$	=	soil internal friction angle
		μ	=	pipe–soil interface frictional coefficient
		L	=	length of pipe
		D_e	=	outer diameter of pipe
		γ	=	unit weight of soil
		K	=	lateral earth pressure, 1
		K_2	=	thrust coefficient of soil acting on pipe, 0.3
		b	=	influencing soil width above pipe

Table 2. The influences of operation parameters on jacking forces.

Operation Parameters	Influence on the Jacking Forces	References
Lubrication	Reduction in frictional force	[11,13,14]
Stoppage	Increase in frictional static resistance	[13,15]
Progress drive length	Increase in frictional force	[3,16,17]
Jacking speed	Increase in face pressure force	[15,17–19]

Although the influences of these operation parameters are identified, the quantitative measurements of these operation parameters on jacking forces remain absent. Recent research has shown the use of machine learning and deep learning techniques in the pipe jacking process, such as predicting the changes in geological conditions [26–29], changes in ground settlement [30–35] and prediction of various operation parameters [36–40]. Hence, this paper will use deep learning techniques, such as gated recurrent units (GRUs) with an attention mechanism, to predict jacking forces through a region of weathered phyllite based on pipe jacking operation parameters as the input features. The model evaluates prediction performances and visualises the contribution of operation parameters to the jacking forces, the specifics of which will be discussed hereinafter.

3. Project Background

A pipe jacking drive spanning 120 m through weathered phyllite drive was performed using the Iseki Unclemole Super TCS 1500. This paper proposes two approaches used for assessing jacking forces in weathered phyllite through pressuremeter tests for the rock strength parameters and a deep learning model using field-measured operation parameters. The location of the pipe jacking drive is shown in Figure 2.

Figure 2. Location of pipe jacking drive through the phyllite drive in Kuching city.

Figure 3 shows the field measured data of ten (10) pipe jacking operation parameters used to train the deep learning model and predict the jacking forces. The inputs of operation parameters consist of operator-dependent decisions (jacking speed, lubricant, cumulative lubricant, slurry bypass pressure, and cutter torque) with responses from the pipe jacking machine (drive progress, days, cumulative days, face slurry pressure, and minimum thrust load).

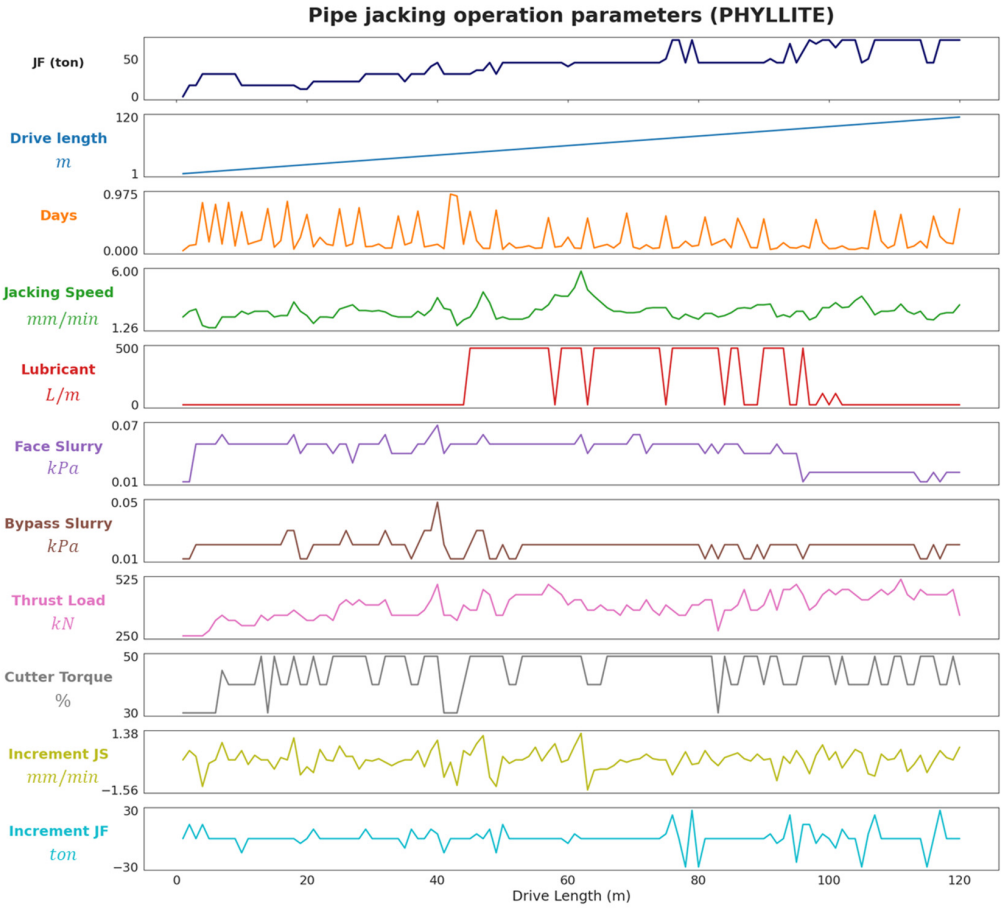

Figure 3. Field-measured operation parameters on jacking forces in weathered phyllite.

4. Methodology

Utilising rock strength properties through *in situ* pressuremeter tests and integrating pipe jacking operation parameters with a deep learning model incorporating an attention mechanism, this paper presents a novel methodological framework for evaluating the jacking forces in a phyllite drive, as illustrated in Figure 4.

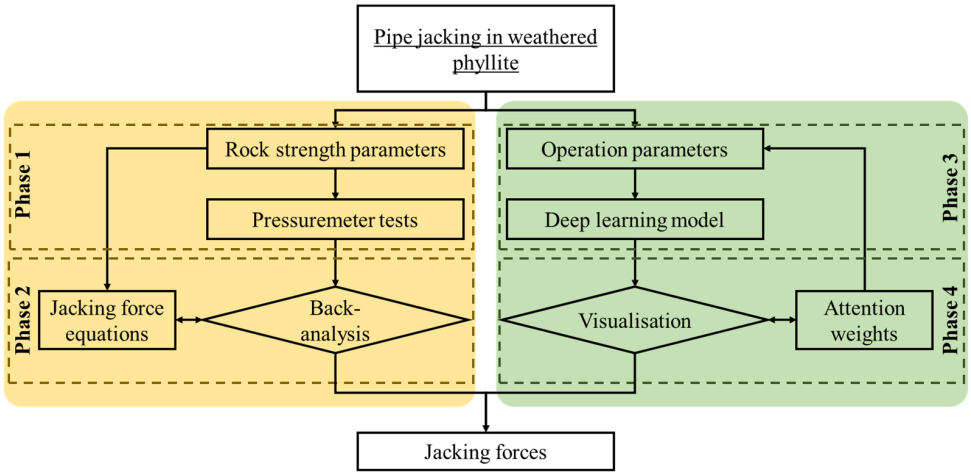

Figure 4. Methodological framework of evaluating jacking forces in weathered phyllite. Yellow section indicates the framework of using *in-situ* pressuremeter test, and green section indicates the framework of using deep learning approach.

4.1. Cavity Expansion Theory and Pressuremeter Testing

An *in situ* test using a pressuremeter (PMT) was introduced to study the strength properties and stiffness of lithology by expanding the probe using pressurised gas or water, which is commonly used for the applications of foundation design [41,42], determining the bearing capacity of the pile [43] and settlement predictions [41]. The PMT was utilised by lowering the probe into the test borehole at the required test depth [44]. Pressure and deformation of the geomaterial were measured during the expansion of the probe, which were subsequently interpreted to characterise the strength properties. Figure 5 shows the PMT results obtained from weathered phyllite.

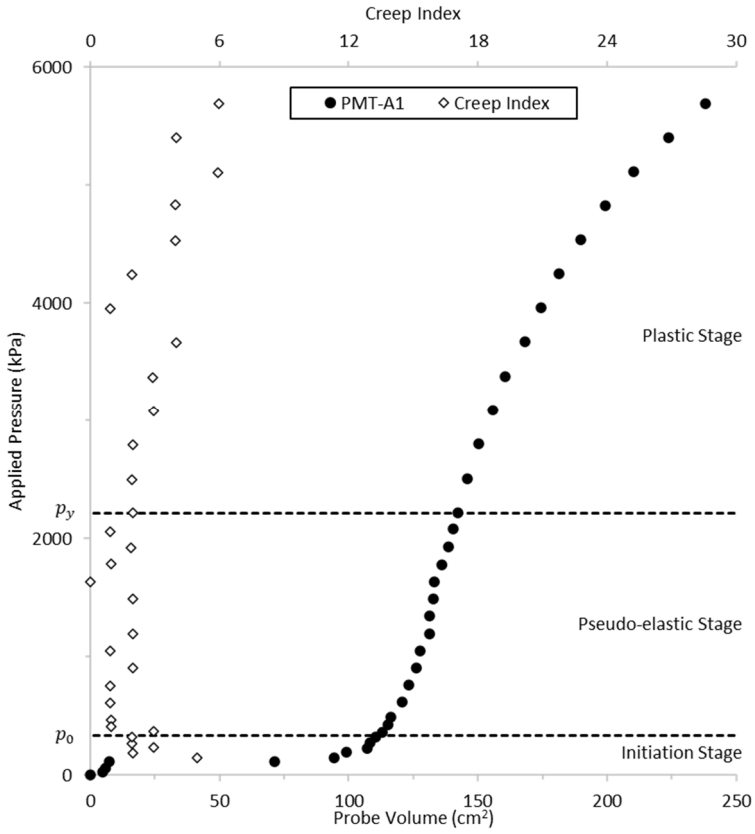

Figure 5. Pressuremeter test results from weathered phyllite [21].

The PMT curve was plotted using the corrected probe pressure against the corrected probe volume, including creep indices, to identify the PMT testing stages. $Creep\ Index = V_{60} - V_{30}$, were calculated using the volume readings taken at 30 s and 60 s for each increment of 100 kPa at 1 min intervals [21]. PMT testing stages can be observed from the creep indices where minimal creep indicates elastic deformations (pseudo-elastic stage), which is significant for calculating pressuremeter modulus, $E_{PMT} = 2(1+v)(V_0 + V_m)\frac{\Delta P}{\Delta V}$, where v = Poisson's ratio, V_0 = volume of the uninflated probe, $\frac{\Delta P}{\Delta V}$ = gradient of the pseudo-elastic stage, V_m = corrected volume reading at the midpoint of linear line in pseudo-elastic stage (linear stress–strain result).

To characterise the strength properties of weathered phyllite from the measured PMT results, an analytical approach based on cavity expansion theory was developed to derive equivalent Mohr–Coulomb (MC) strength properties [45]. Since the initiation stage of the PMT result does not represent the true pressure-expansion behaviour of weathered phyllite, modification of the measured PMT result was performed by shifting the deformation axis to omit this initiation stage from the subsequent analysis, as shown in Figure 6. The circumferential strain, ε_θ, was calculated $\varepsilon_\theta = \frac{a - a_0}{a_0}$, where $a = cavity\ radius$, and $a_0 = initial\ cavity\ radius$ [21]. The theoretical pressure–expansion curve based on cavity

expansion theory will be calibrated with the measured PMT result by plotting ε_θ as the deformation axis.

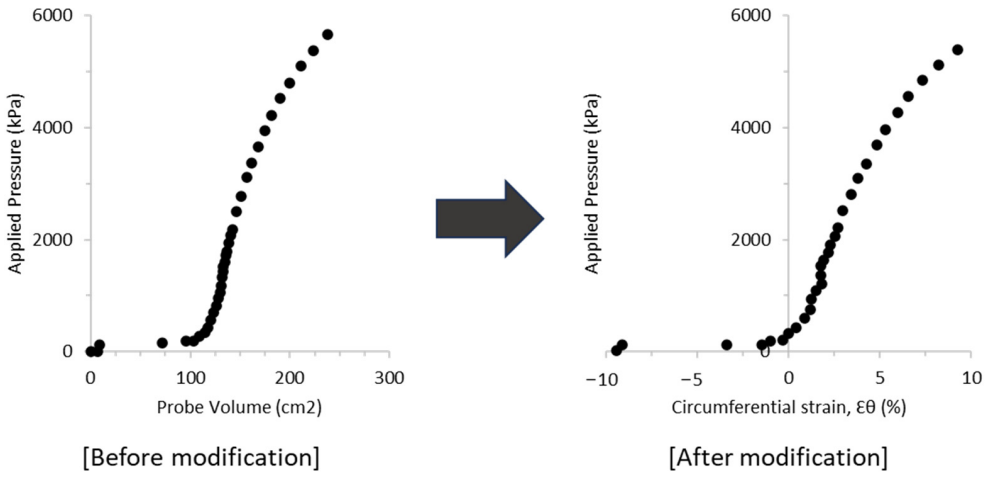

Figure 6. Modification of pressuremeter test result on the deformation axis [21].

Cavity expansion theory was used to optimise the theoretical pressure–expansion curve that fits the measured pressuremeter test result [45]. This allowed for the characterisation of rock strength properties via an equivalent Mohr–Coulomb (MC) strength parameters (c' and φ') [21]. Table 3 shows a series of equations developed to generate a theoretical pressuremeter pressure–strain curve based on cavity expansion theory [45].

Table 3. Equations used to generate theoretical pressuremeter pressure–strain curve based on cavity expansion theory [45].

Shear Modulus	Function of Material Properties	Function of Cohesion and Friction Angle	Function of Friction Angle	Function of Dilation Angle
$G[MPa] = \frac{E}{2(1+\nu)}$	$M[MPa] = \frac{E}{1-\nu^2}$ $\gamma\ [-] = \frac{\alpha(\beta+1)}{(\alpha-1)\beta}$ $\delta\ [-] = \frac{\gamma+(\alpha-1)p_o}{2(\alpha+1)G}$ Where: p_0 = in-site pressure, derived from creep index plot $\eta\ [-] = e^{\frac{(\beta+1)(1-2\nu)[Y+(\alpha-1)p_o][1+\nu]}{E(\alpha-1)\beta}}$ $\xi\ [-] = \left[\frac{2(1-\nu^2)\delta}{(1+\nu)(\alpha-1)\beta}\right]\left[\alpha\beta+1-\frac{\nu(\alpha+\beta)}{1-\nu}\right]$	$Y\ [-] = \frac{2c\cos\varnothing}{1-\sin\varnothing}$	$\alpha\ [-] = \frac{1+\sin\varnothing}{1-\sin\varnothing}$	$\beta\ [-] = \frac{1+\sin\psi}{1-\sin\psi}$ where ψ = dilation angle

Young's modulus, E, determined from the PMT modulus, E_{PMT}, Poisson's ratio, ν and MC rock strength properties, cohesion, $c\prime$ and friction angle, $\varnothing\prime$, were considered for the equations to obtain the theoretical pressure–expansion curve. The MC strength parameters were interpreted from the theoretical pressure–expansion curve that fitted from the beginning of the plastic stage.

4.2. Development of Rock Strength Parameters for Back-Analysis of Jacking Forces

The developed MC strength parameters from PMT were applied to the frictional jacking force model developed by Pellet-Beaucour and Kastner [17]. Measured jacking forces were used to back-analyse the frictional coefficient, μ. Table 4 shows the expressed equation from the developed frictional jacking force model to suit the back-analysis.

Table 4. Frictional jacking force model for back-analysis of jacking forces.

Frictional Jacking Force Model	Expressed Jacking Force Model
$F = \mu L D_e \frac{\pi}{2}\left[\left(\sigma_{EV} + \frac{\gamma D_e}{2}\right) + K_2\left(\sigma_{EV} + \frac{\gamma D_e}{2}\right)\right]$ $\sigma_{EV} = \frac{b\left(\gamma - \frac{2C}{b}\right)}{2K\tan\emptyset}\left(1 - e^{-2K\tan\emptyset\frac{h}{b}}\right)$ $b = D_e\left[1 + 2\tan\left(\frac{\pi}{4} - \frac{\emptyset}{2}\right)\right]$	$\mu = \frac{F/L}{D_e\frac{\pi}{2}\left[\left(\sigma_{EV} + \frac{\gamma D_e}{2}\right) + K_2\left(\sigma_{EV} + \frac{\gamma D_e}{2}\right)\right]}$ Where: F/L = measured jacking forces

F = jacking forces; μ = friction coefficient; L = length of pipe; D_e = outer diameter of pipe; γ = unit weight of soil; K = coefficient of lateral earth pressure = 1; K_2 = thrust coefficient acting on pipe = 0.3; σ_{EV} = soil stresses due to arching acting on pipe crown; h = soil cover depth from ground level to the pipe crown; b = influencing soil width above the pipe; C = cohesion; $\emptyset$ = friction angle (in degrees).

4.3. Deep Learning Technique for Predicting Operation Parameters

During pipe jacking construction, field-measured operation data were collected. The raw handwritten data were digitised and normalised to train the deep learning model, namely the gated recurrent unit (GRU). GRUs have the ability to handle long sequential data, such as the aforementioned measurements of pipe jacking operation parameters. The prediction performance from the model will be evaluated by calculating the R^2 values between the predicted and ground truth jacking forces. Subsequently, visualisation of the attention to the respective operation parameters for the prediction of jacking forces will be discussed. Table 5 shows the studies in the literature where machine learning (ML) and deep learning (DL) have been applied to various objectives in tunnelling.

Table 5. Past studies on ML and DL techniques used in tunnelling.

Authors	ML/DL Techniques Used *	Objective		
		Prediction of Geological Conditions	Prediction of Changes in Ground Settlement	Prediction of Operation Parameters
[26]	SVM	✔		
[36]	LSTM			✔
[37]	RNN, LSTM			✔
[38]	RNN			✔
[39]	ANNs, GA-ANNs			✔
[27]	ANNs, LSTM	✔		
[30]	ANNs, LSTM, GRU, Conv1d		✔	
[28]	GCN, LSTM	✔		
[40]	ANNs, LSTM			✔
[29]	RF, SVM, AdaBoost	✔		
[20]	GRU, Attention mechanism			✔

* SVM = support vector machine; LSTM = long short-term memory; RNN = recurrent neural network; ANNs = artificial neural networks; GA-ANN = hybrid genetic algorithm optimised ANNs; GRU = gated recurrent unit; Conv1d = 1D convolutional neural networks; GCN = graph convolutional network; RF = random Forest.

ML and DL techniques can understand the complicated behaviour of underground soils and rocks [23]. The past studies shown in Table 5 used tunnelling operation parameters (jacking speed, cutter torque, etc.) as input features to predict the changes in jacking forces. However, the prediction accuracy depends on geological conditions that are fairly homogenous, which was not the case in the weathered lithology from the current study. Furthermore, the contributions of the respective input features (i.e., tunnelling operation parameters) towards the predicted features were not discussed. In the current study, we will use an attention mechanism to identify the significance of inputs on the prediction. This will be achieved through the visualisation of the attention weightage assigned to each input to achieve the prediction of jacking forces.

Deep neural networks have often been characterised as a black box model [23,46,47]. Despite their success in matching input data to output prediction, limited work has been

conducted to explore the underlying features influencing predictions related to pipe jacking forces. Such insights would not only uncover the black box, they could also potentially allow interpretation of the deep learning networks through verification against human understanding.

An attention mechanism was introduced to explain the influential features derived from the prediction of the deep learning networks. Incorporating attention mechanisms represents a technique that guides deep learning models toward the most suitable features during prediction. It has been widely used in applications such as computer vision and speech processing [48–51]. In geotechnical engineering, variable and uncertain geological environments can cause challenges during the operation of the tunnelling process [52–54]. Although deep learning models used in tunnelling such as RNN, LSTM, GRU, and Conv1D [36,37,47,55–57] show the ability to handle such complex data, they do not provide insights into which features of the data have the most influence on the predictions. By applying the attention mechanism in the deep neural networks, it can effectively learn to focus on specific features that are significant to the prediction, addressing the challenges caused by heterogeneous geological conditions during the prediction such as jacking forces [20,39,58], controlling the alignment of the machine [55], and ground settlement [30]. Thus, the coupling of attention mechanism can align the insights of deep neural networks with human expertise and geological understanding.

Figure 7 compares the prediction accuracy of the proposed global-attention-mechanism-based LSTM network with the conventional LSTM network to predict the lithology in shield tunnelling [56]. In addition, the improvement in prediction using the attention mechanism has been validated by comparing the ground truth jacking forces with the predicted jacking forces [20]. This concluded that the attention mechanism can further improve the deep learning model prediction performance. However, visualising the model using attention mechanisms remains relatively unexplored.

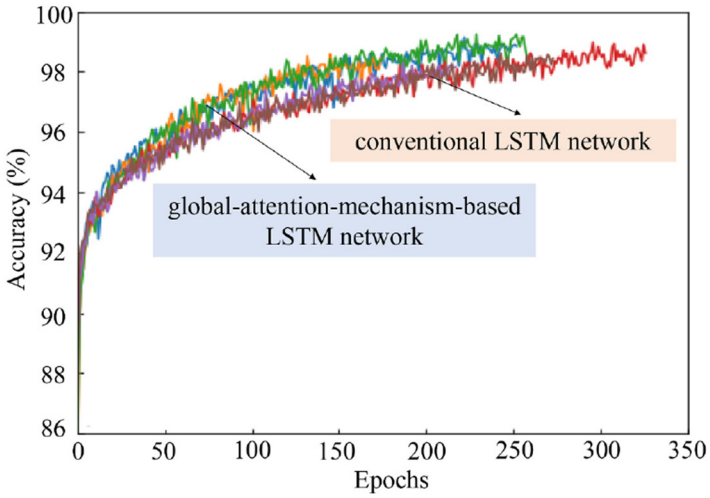

Figure 7. Accuracy curves of global-attention-mechanism-based LSTM network against conventional LSTM network to predict lithology in TBM tunnelling [56]. Upper curve indicates the global-attention-mechanism-based LSTM network which shows better accuracy than the lower curve of the conventional LSTM network.

Therefore, the current study will be utilising attention mechanism to locate the important features of pipe jacking operation parameters, which capture the relationship among multivariate variables spanning across the drive length, ultimately enhancing the prediction of jacking forces.

4.4. Feature Visualisation of Operation Parameters through Attention Mapping

Attention-based RNN models were chosen due to their ability to handle sequential data. GRU, which is a type of RNN, was used to better understand the influence of pipe jacking operation parameters on jacking forces. The GRU enables faster learning with less

data when compared to other deep learning techniques, such as LSTM [30]. Furthermore, GRU has been previously applied for predicting jacking forces [20,59]. Figure 8 shows the comparison of using different deep learning models (GRU, LSTM, Conv1D) when predicting the jacking forces in this weathered phyllite. It is clearly shown that the GRU model outperformed the other deep learning models with an R^2 of 0.82, showing that the model was able to handle limited data [30,60,61].

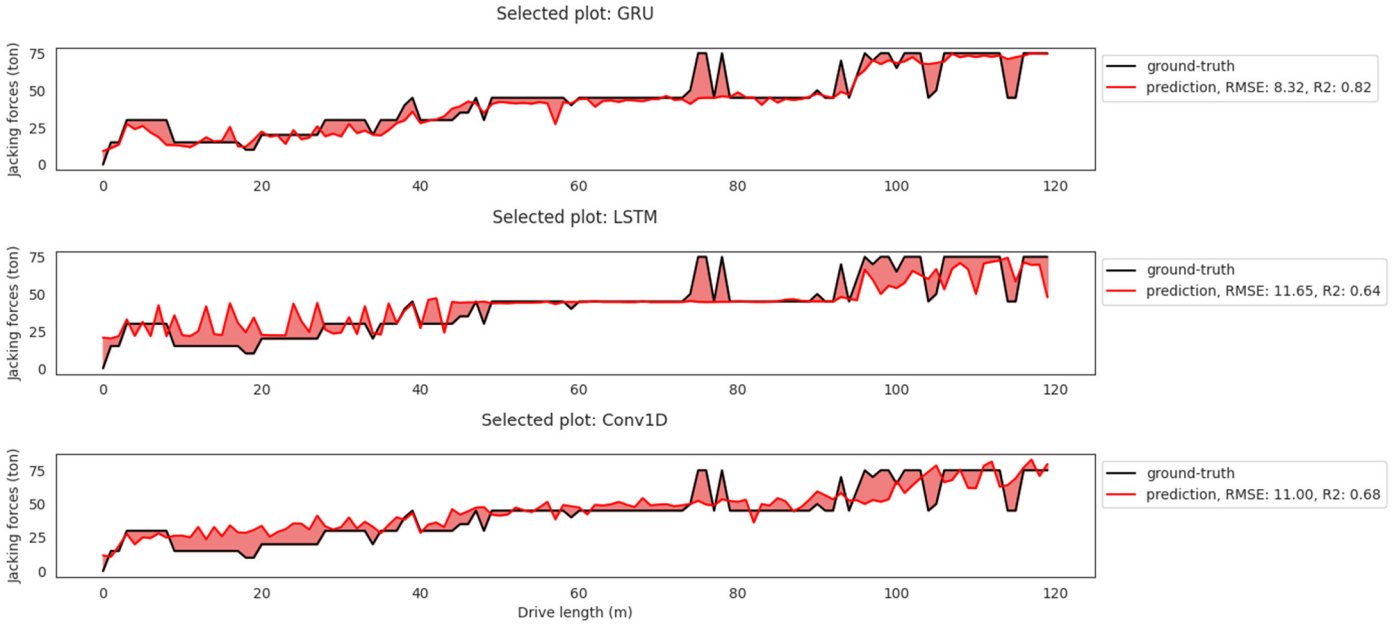

Figure 8. Comparison using different deep learning models to predict the jacking forces in weathered phyllite.

Figure 9 shows the comparison of the jacking force (JF) prediction performance of GRU with attention and without attention. It can be seen that the attention mechanism in the deep learning model resulted in an R^2 of 0.82 compared to the model without the attention mechanism, which demonstrated an R^2 of 0.77. This implied that the attention mechanism can effectively capture the significant input features, resulting in enhanced prediction of jacking forces. The prediction of jacking forces was evaluated using R^2 by training the attention-based GRU model using field-measured pipe jacking operation parameters, which will be discussed hereinafter.

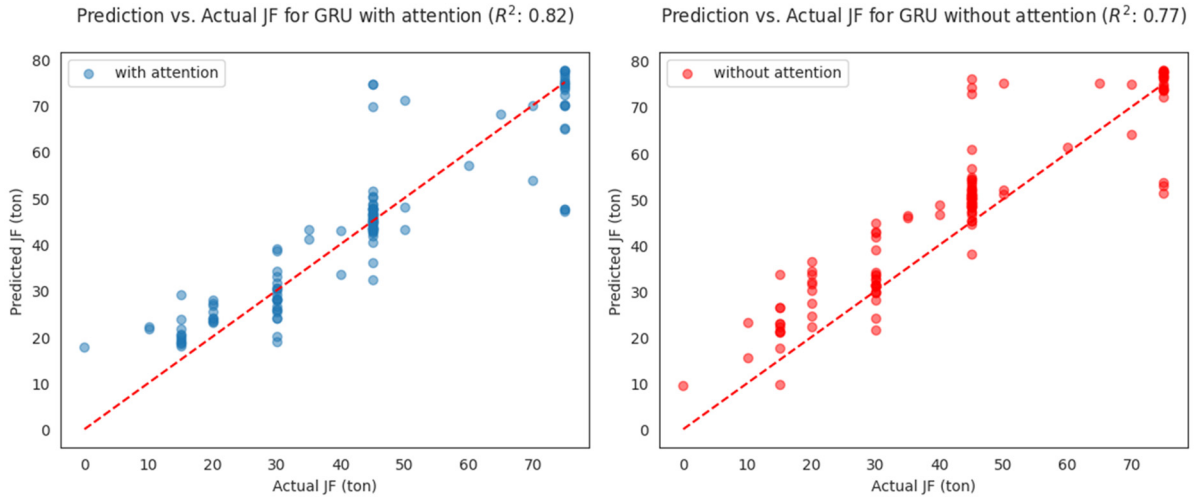

Figure 9. Comparison of GRU model prediction performance with and without attention mechanism.

Figure 10 shows insight into the deep learning model using GRU with an attention mechanism used in previous studies to predict jacking forces using pipe jacking operation parameters [20]. The data will be pre-processed by normalising between 0 and 1 before being fed into the model. Thus, all the data fed into the model are given equal importance (same scale across all the features) without being affected by their original scale measurement (different scales from different features).

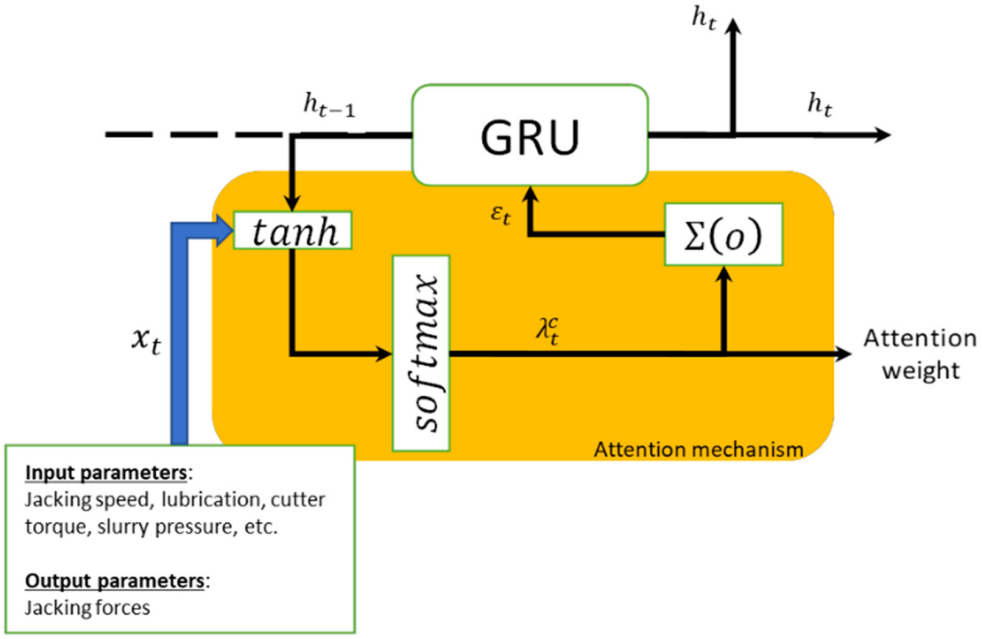

Figure 10. Schematic diagram of GRU model with attention mechanism [20].

The input features (x_t) from the collected pipe jacking operation parameters will be fed into the GRU model incorporating the attention mechanism with the previous hidden states (h_{t-1}) to generate a new hidden state (h_t). The model will continue with this process by updating the previous data with current input features until the end of the prediction step. Within the attention mechanism, the attention weight (λ_t) was calculated based on the input features (x_t), to determine the weighted average of the features (ε_t). The attention function $f : x_t, h_{t-1} \rightarrow \varepsilon_t$ is defined as follows:

$$\zeta_t = \{\tanh(x_t W_x + h_{t-1} W_h)\} W_a \quad (1)$$

$$\lambda_t = softmax(\zeta_t) \quad (2)$$

$$\varepsilon_t = \sum \lambda_t x_t \quad (3)$$

This paper proposes a deep learning model incorporating attention mechanism, as shown in Figure 11, which has the ability to quantify the attention of each input feature at each time step ($Input_t$) on the prediction ($Output_t$) using the attention mechanism.

The integration of the attention mechanism is aimed not only at improving the model prediction performance, but also at facilitating the visualisation of the significance of features contributing to the prediction of jacking forces. This can further help to understand the importance of each operation parameter contributing to the jacking forces by extracting the attention weights obtained with respect to each individual input (operation parameters) from the model. The model was trained using a dataset of 120 data points which covered the entire drive length of 120 m. The dataset was equally divided into five sections. In each section, 80% of the data were used for training while the remaining 20% were used for testing [20]. The model and the hyperparameters used in this study are shown in Table 6 below.

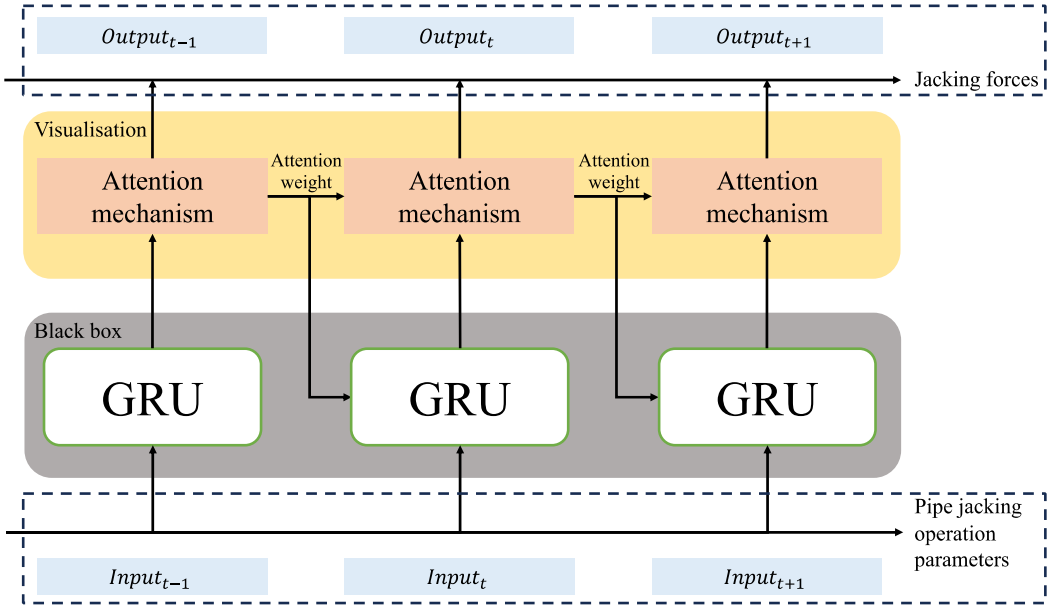

Figure 11. Proposed attention-based GRU model.

Table 6. Parameters used in this study.

Parameters	Specification
Recurrent neural network type	Gated recurrent unit (GRU)
Attention mechanism type	Bahdanau Attention
Layers	2
Neurons	100
Epochs	50
Step size	10
Batch size	1
Activation	Rectified Linear Unit (ReLU)
Training set	80%
Testing set	20%

5. Results

5.1. Back-Analysis of Jacking Forces

An *in situ* pressuremeter test was carried out at a depth of 15 m in weathered phyllite. Figure 12 shows the result of the *in situ* pressuremeter test performed in accordance with ASTM D4719-07 [62], and the theoretical pressure–strain curve.

The theoretical pressuremeter pressure–strain curve was calculated using a series of equations based on the cavity expansion theory developed by [43,45]. The Mohr–Coulomb parameters (rock strength properties) of cohesion, $C\prime$, and internal friction angle, $\varnothing\prime$, were obtained from pressuremeter results with cavity expansion theory to back-analyse the jacking forces in the weathered phyllite drive. Table 7 shows the rock strength properties calculated from the pressuremeter test based on the cavity expansion theory.

The frictional jacking force model developed by Pellet-Beaucour and Kastner [17] will be used for back-analysis using strength properties obtained from the cavity expansion theory. Furthermore, the model assumes a linear relationship between drive length and jacking forces, which prompts the plot of best fit (linear trend) for field-measured jacking forces. Thus, measured jacking forces from the best fit line show the forces increased at a rate of 4.8 kN/m, as shown in Figure 13, which will be used to back-analyse the frictional coefficient.

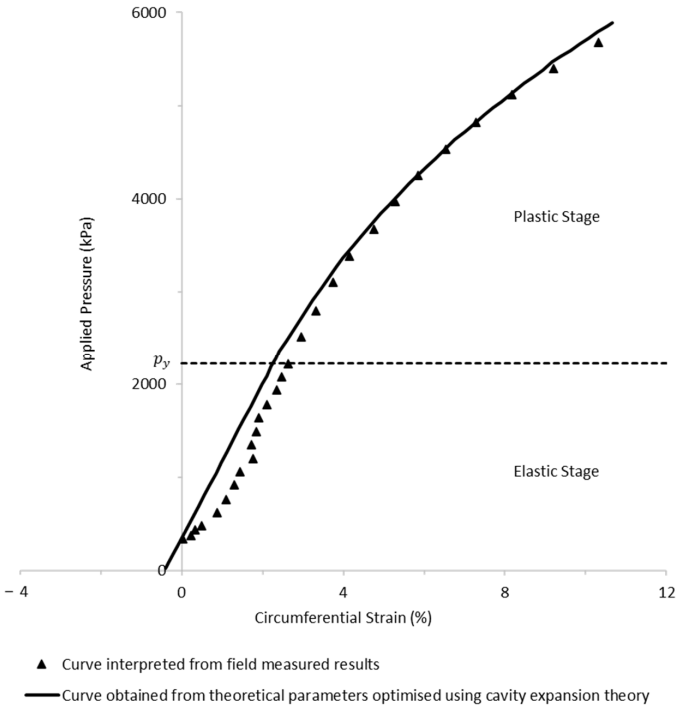

Figure 12. Pressuremeter test results with theoretical curve based on the cavity expansion theory.

Table 7. Strength properties derived from the cavity expansion theory.

Strength Properties from Cavity Expansion Theory	Values
Young's modulus, E	173 MPa
Poisson's ratio, ν	0.3
Cohesion, $C\prime$	3.6 MPa
Friction angle, $\varnothing\prime$	53°

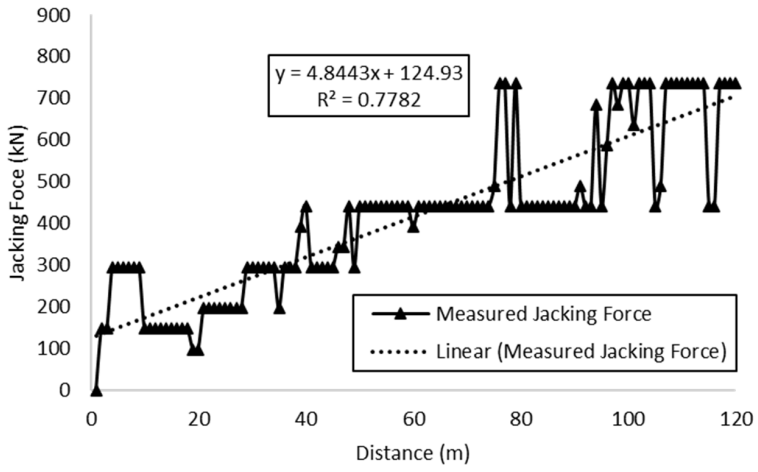

Figure 13. Measured jacking forces with line of best fit in weathered phyllite.

For the back-analysis, the MC strength parameters interpreted from the pressuremeter testing will be applied to the Pellet-Beaucour and Kastner model [17]. Table 8 shows the results of back-analysis of the jacking forces, with the back-analyzed μ compared against $\mu < 0.3$ for lubricated drives [11,58,63].

The back-analyzed frictional coefficient for the highly weathered phyllite drive was 0.08, which was less than the threshold of 0.3 for well-lubricated drives. This was further

validated by the volume of injected lubricant (181 L/m) into the theoretical overcut volume (113 L/m), which showed a lubricant utilisation ratio of 1.6, indicating the injected lubricant had fully occupied the overcut region without significant loss of lubrication.

Therefore, the interpreted strength properties from pressuremeter testing were able to perform back-analysis of frictional jacking forces in weathered phyllite through a mechanistic approach. Nevertheless, the influences of the pipe jacking operation parameters on jacking forces remain uncertain. Hence, the influences of these operation parameters on jacking forces in weathered phyllite will be visualised and discussed using deep learning with an attention mechanism.

Table 8. Results from back-analysis of jacking forces.

External Pipe Diameter, D_e	**1.78 m**
Effective overburden pressure, $\sigma\prime_v$	162 kPa
Best fit linear regression of measured jacking force, JF_{meas}	4.8 kN/m
Cohesion, $C\prime$	3600 kPa
Friction angle, $\varnothing\prime$	53.0°
Friction coefficient, μ	0.08 < 0.3

5.2. Attention Mapping of Operation Parameters

Figure 14 shows the attention allocated for each input feature of operation parameters on the prediction of jacking forces in weathered phyllite. This process provides insights into pipe jacking construction, highlighting the significance of operation parameters on jacking forces.

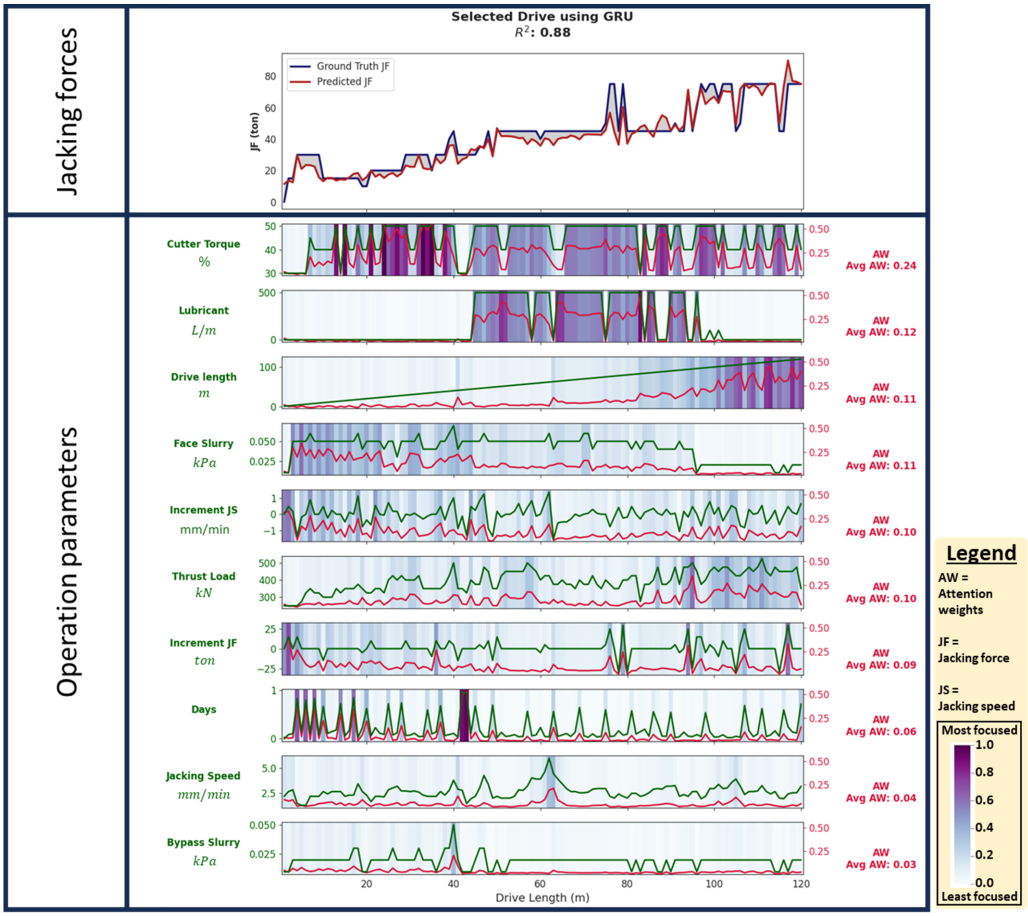

Figure 14. Attention allocated for each input feature on jacking forces in weathered phyllite.

6. Discussion

Generally, it was observed that cutter torque received the most attention (0.24) followed by lubricant, drive length, face slurry, incremental jacking speed (i.e., jacking acceleration), thrust load and incremental jacking force, respectively. For these latter operation parameters, the average attention weightages were quite similar, ranging between 0.09 and 0.12. The remaining input features (i.e., days, jacking speed and bypass slurry pressure) received minimal attention, with attention weightages ranging between 0.03 and 0.06. Detailed discussions of these attention weightages will be described hereinafter.

6.1. Influence of Operation Parameters at Micro-Tunnel Boring Machine (mTBM) Face

Cutter torque, thrust load and face slurry pressure are the operation parameters measured at the face of the mTBM. Cutter torque is related to the rotational resistance of the cutter face. Thrust load is measured from a load cell located behind the cutter face [58,64]. Face slurry pressure is applied to remove loose excavated rock spoil away from the tunnel face.

Based on the attention results shown in Figure 14, it was observed that cutter torque received more attention compared to thrust load and face slurry pressure. Cutter torque values generally ranged between 40% and 50%. Despite this, there were two distinct patterns in attention. Attention towards cutter torque increased during instances when cutter torque experienced sudden increases up to attention values of 0.50, for example at drive sections from 25 m to 40 m, and from 80 m to the end of the drive. From 40 m to 80 m, the attention was fairly consistent at approximately 0.25, owing to the minimal variations in cutter torque. Thrust load was minimally attended, with attention values generally reaching only up to 0.20. Greater attention was observed from 90 m to the end of the drive. This coincided with significant fluctuations in jacking forces between 45 tons and 70 tons. While the attention of cutter torque and thrust load fluctuated throughout the drive, face slurry pressure tended to reduce gradually throughout the drive. Face slurry pressure was generally maintained at 0.050 and 0.040 up to 100 m, beyond which the face slurry pressure reduced to 0.020. The attention values reduced from 0.050 at the start of the drive down to almost 0 at the end of the drive, indicating that the slurry face pressure was contributing less and less to the jacking forces as the drive progressed.

As discussed in the previous section, the jacking force is made up of two components, which are the face pressure and frictional force along the pipeline. Ideally, the face pressure should be kept constant when driving through the same lithology throughout the design span. With the face pressure being kept constant, frictional force would eventually become more important than face pressure as drive length increases. Nonetheless, at the beginning of the drive, where frictional force was yet to be accumulated, the face pressure would contribute to most of the jacking force. The deep learning model with attention mechanism was able to show similar findings by focusing initially more on the face mTBM parameters.

Apart from that, it was also found that the face mTBM parameters were being focused more than other parameters, such as jacking speed and lubricant injected. The rankings of importance level for cutter torque, face slurry pressure and thrust load were as follows: first place, third place and fourth place, respectively. This finding was obtained because this phyllite drive was a well-lubricated drive, having a lubricant utilisation ratio of 1.6. Hence, frictional force was well-controlled. More attention would be given to the face pressure which was partly affected by the face mTBM parameters such as cutter torque, face slurry pressure and thrust load.

6.2. Influence of Jacking Speed on Jacking Force

The attention results for jacking speed in phyllite drive are shown in Figure 15, with the blue line indicating the jacking speed and the orange line indicating attention weights.

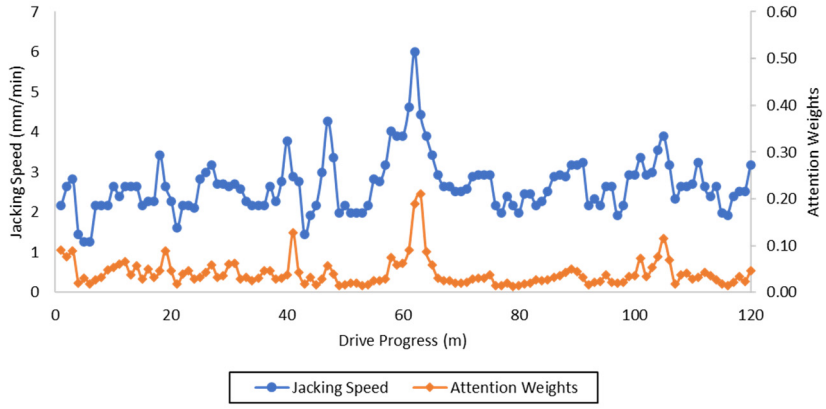

Figure 15. Measured jacking speed against its attention weights.

Overall, the jacking speed in the phyllite drive was not heavily focused. The model focused only on jacking speed when it was extraordinarily high, as observed at the drive length of 62 m in Figure 15.

Jacking speed is an important operation parameter during the pipe jacking operation as it governs the duration required to complete a drive. In ideal conditions, jacking speed should be high to reduce the construction period. On the other hand, a high jacking speed would lead to a dramatic increase in the jacking force, elevating the risks of sinkholes or pipe ruptures. The model suggested that the jacking speed should be given extra attention when a higher jacking speed is applied for transversing through phyllite. This observation matches the findings from [11], where it is mentioned that in phyllite drives, increases in jacking speed would not cause significant changes in the jacking force.

6.3. Influence of Lubricant on Jacking Force

As discussed in the previous section, the injection of lubricant reduces the frictional resistance along the pipeline through the introduction of uplifting force to the pipe and hence, reducing the contact area between the pipeline and surrounding soil [65]. Ideally, the overcut space, which is the space between the pipeline and soil, should be entirely filled with lubricant. Hence, the volume of lubricant injected should be the same as the theoretical overcut volume. Having more lubricant injected than the theoretical volume while jacking force is not instantaneously reduced could possibly represent that there is a loss of lubricant through the fissures to the surroundings. Such a situation shows that the lubrication is ineffective.

The lubrication performance can be assessed by computing the utilisation ratio [21], which is to find the ratio of average lubricant injected to the theoretical overcut volume as shown below. Obtaining a lubricant utilisation ratio that is significantly higher than one could represent that there is a significant loss of lubricant to the surroundings, instead of being utilised to reduce the jacking force.

$$\text{Lubricant Utilisation Ratio} = \frac{\text{Average injected lubricant volume}}{\text{Theoretical overcut volume}} \quad (4)$$

Figure 16 shows the plot of the volume of lubricant injected at each drive length (in blue) with attention weights (in orange). The theoretical overcut volume for this drive was 113 L/m (in red), with an allowance of 20 mm clearance between the pipelines and the outer diameter of the mTBM. The average lubricant injected computed was 181 L/m (in green). Thus, the lubricant utilisation ratio obtained was 1.6, indicating that the overcut space is entirely filled by the lubricant without having any major loss of lubricant. The effective lubricant performance is also reflected in the jacking force, where the highest recorded jacking force for this drive was 75 tons, without having a significant increase in jacking force, as shown in Figure 14.

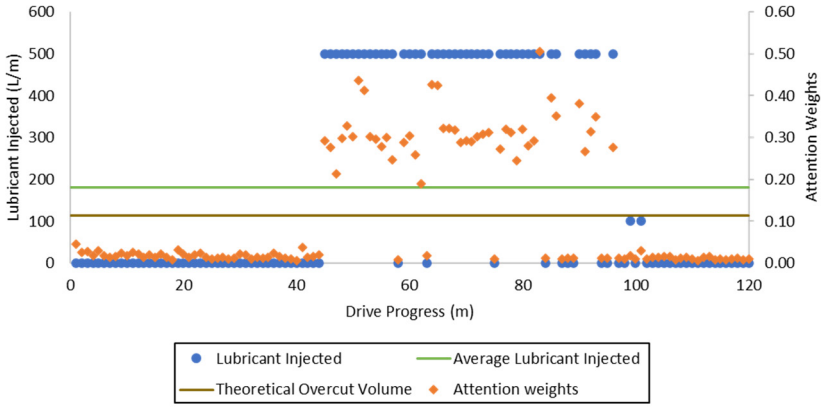

Figure 16. Measured lubricant injected against its attention weights with theoretical volume and average lubricant injected.

The results showed that the deep learning model focused on this operation parameter when the instantaneous lubricant utilisation ratio at a drive length is higher than one (the volume of lubricant injected was more than the theoretical overcut volume). Such a situation can be observed at a drive length of 45 m to 96 m, where the majority of the volume of lubricant injected was 500 L/m. In contrast, at the drive length of 99 m and 101 m where the lubricant injected was 100 L/m, the lubricant is not paid much attention by the model.

Lubricant injected was not given high attention weights by the deep learning model as compared to other operation parameters (parameters related to face mTBM), showing that lubricant is comparatively less important in phyllite drives. This observation matched the findings from [3], where phyllite was found to be characteristically bedded and tightly folded. Such geological characteristics form a water-tight and stable bore to trap the lubricant in the overcut region, instead of dissipating it to the surrounding geology. Hence, in the phyllite drive, frictional force along the pipeline was well-controlled, making a limited contribution to the jacking force. Such findings were validated by back-analysing the friction coefficient of 0.08 for phyllite drive [11,65], which is lower than the suggested range of friction coefficient (0.1–0.3) for a well-lubricated drive by [63], indicating that this was a well-lubricated drive.

7. Conclusions

This paper successfully uses two approaches, namely a mechanistic approach utilising pressuremeter testing and a deep learning approach with an attention mechanism for the assessment of jacking forces in weathered phyllite. The conclusions in this paper can be drawn as follows:

(1) The pressuremeter testing was implemented to develop equivalent rock strength properties ($C\prime$ and $\varnothing\prime$) based on cavity expansion theory, which will be used for back-analysing the frictional jacking forces model developed by Pellet-Beaucour and Kastner [17] on the friction coefficient.

(2) The back-analysed friction coefficient using rock strength properties identified that the selected pipe jacking drive in weathered phyllite was well-lubricated. Furthermore, the discussed method using the pressuremeter test for the mechanistic approach was validated for back analysis on jacking forces in 'soft rock' [11,14].

(3) The influences of pipe jacking operation parameters on jacking forces were visualised using the attention-based GRU model with an accuracy of 88%. From the overall analysis, the attention focused on the cumulative parameters, such as drive length, cumulative days and cumulative lubricant injected, became increasingly significant as the drive progressed.

(4) The cumulative parameters contribute significantly to jacking forces. When the total number of days increases, it produces higher static frictional resistance along the pipes.

When the pipe jacking progressed, the drive lengths increased, which caused higher frictional resistance pushing from the opposite direction, requiring larger jacking forces to overcome.

(5) The operation parameters from the cutter face, such as thrust load, cutter torque and face slurry pressure, became less significant as the pipe jacking progressed. This observation is reasonable, considering the weathered phyllite has stable bore conditions, in which the jacking forces are more likely to be influenced by the increased friction along the surface of the pipe than the activities at the tunnel face.

To conclude, it is challenging to extract intact phyllite cores from highly weathered formations for the purpose of laboratory strength testing. To overcome this challenge, previous studies had reconstituted phyllite spoil using direct shear apparatus [11], while this paper highlights the potential of using pressuremeter testing to develop equivalent rock strength properties. Moreover, the significance of pipe jacking operation parameters has been effectively visualised and discussed using an attention-based deep learning model.

The findings of the development of MC parameters from cavity expansion theory established using the pressuremeter test are transferable to other geological conditions, which have been established by Yu and Houlsby [45]. The main limitation here is the maximum expansion pressure the pressuremeter test can reach when dealing with significantly stronger rock masses [44]. Additionally, the use of GRU with an attention mechanism is applicable to pipe jacking drives in other geological conditions, which could potentially highlight changes in the importance of operation parameters on jacking forces in other geological conditions.

Author Contributions: Writing—original draft preparation, formal analysis, investigation, methodology, L.Y.Y.; formal analysis, F.P.; visualization and writing—original draft preparation, P.G.K.; conceptualization, methodology, writing—review and editing and supervision, C.S.C. and S.H.L.; writing—review and editing and supervision, D.Z.; methodology, supervision and writing—review and editing, D.E.L.O. All authors have read and agreed to the published version of the manuscript.

Funding: This research received no external funding.

Data Availability Statement: The data that has been used is confidential.

Acknowledgments: The authors would like to thank Hock Seng Lee Bhd and Jurutera Jasa (Sarawak) Sdn Bhd for making this work possible.

Conflicts of Interest: Author Fredrik Phangkawira was employed by the company WSP Golder. The remaining authors declare that the research was conducted in the absence of any commercial or financial relationships that could be construed as a potential conflict of interest.

References

1. Sewerage Services Department Sarawak Operation of Kuching Centralised Sewage Treatment Plant. Available online: https://ssd.sarawak.gov.my/web/subpage/webpage_view/361 (accessed on 30 November 2023).
2. Tan, D. *Geology of the Kuching Area, West Sarawak*; Geological Survey of Malaysia: Kuching, Malaysia, 1993.
3. Choo, C.S.; Ong, D.E.L. Impact of Highly Weathered Geology on Pipe-Jacking Forces. *Geotech. Res.* **2017**, *4*, 94–106. [CrossRef]
4. Bhasin, R.; Barton, N.; Grimstad, E.; Chryssanthakis, P. Engineering Geological Characterization of Low Strength Anisotropic Rocks in the Himalayan Region for Assessment of Tunnel Support. *Eng. Geol.* **1995**, *40*, 169–193. [CrossRef]
5. Gurocak, Z.; Solanki, P.; Alemdag, S.; Zaman, M.M. New Considerations for Empirical Estimation of Tensile Strength of Rocks. *Eng. Geol.* **2012**, *145–146*, 1–8. [CrossRef]
6. Ramamurthy, T.; Rao, G.V.; Singh, J. Engineering Behaviour of Phyllites. *Eng. Geol.* **1993**, *33*, 209–225. [CrossRef]
7. Saroglou, H.; Marinos, P.; Tsiambaos, G. The Anisotropic Nature of Selected Metamorphic Rocks from Greece. *J. S. Afr. Inst. Min. Metall.* **2004**, *104*, 217–222.
8. Tiwari, R.P.; Rao, K.S. Response of an Anisotropic Rock Mass under Polyaxial Stress State. *J. Mater. Civ. Eng.* **2007**, *19*, 393–403. [CrossRef]
9. Shea, W.T.; Kronenberg, A.K. Strength and Anisotropy of Foliated Rocks with Varied Mica Contents. *J. Struct. Geol.* **1993**, *15*, 1097–1121. [CrossRef]
10. Deere, D.U. *Rock Quality Designation (RQD) after Twenty Years*; U.S. Army Corps of Engineers Contract Report GL-89-1; Waterways Experiment Station: Vicksburg, MS, USA, 1989.

11. Ong, D.E.L.; Choo, C.S. Assessment of Non-Linear Rock Strength Parameters for the Estimation of Pipe-Jacking Forces. Part 1. Direct Shear Testing and Backanalysis. *Eng. Geol.* **2018**, *244*, 159–172. [CrossRef]
12. Choo, C.S.; Ong, D.E.L. Assessment of Non-Linear Rock Strength Parameters for the Estimation of Pipe-Jacking Forces. Part 2. Numerical Modeling. *Eng. Geol.* **2020**, *265*, 105405. [CrossRef]
13. Shao, B.; Ma, B.; Shi, L. A Sewer Pipeline Installation Using Pipe-Jacking in Lang Fang. In Proceedings of the ICPTT 2009: Advances and Experiences with Pipelines and Trenchless Technology for Water, Sewer, Gas, and Oil Applications, Shanghai, China, 18–21 October 2009.
14. Shou, K.; Yen, J.; Liu, M. On the Frictional Property of Lubricants and Its Impact on Jacking Force and Soil-Pipe Interaction of Pipe-Jacking. *Tunn. Undergr. Space Technol.* **2010**, *25*, 469–477. [CrossRef]
15. Cheng, W.C.; Ni, J.C.; Shen, J.S.L.; Huang, H.W. Investigation into Factors Affecting Jacking Force: A Case Study. *Proc. Inst. Civ. Eng. Geotech. Eng.* **2017**, *170*, 322–334. [CrossRef]
16. Ji, X.; Zhao, W.; Ni, P.; Barla, M.; Han, J.; Jia, P.; Chen, Y.; Zhang, C. A Method to Estimate the Jacking Force for Pipe Jacking in Sandy Soils. *Tunn. Undergr. Space Technol.* **2019**, *90*, 119–130. [CrossRef]
17. Pellet-Beaucour, A.-L.; Kastner, R. Experimental and Analytical Study of Friction Forces during Microtunneling Operations. *Tunn. Undergr. Space Technol.* **2002**, *17*, 83–97. [CrossRef]
18. Aiman, M.S.; Hadri, M.; Mohamad, H. Case Study of Sewerage Pipe Installation Using Pipe Jacking and Micro-Tunnelling Boring Machine (MTBM) in Ipoh. In *IOP Conference Series: Materials Science and Engineering*; IOP Publishing Ltd.: Bristol, UK, 2020; Volume 932.
19. Staheli, K. Jacking Force Prediction: An Interface Friction Approach Based on Pipe Surface Roughnes. Ph.D. Thesis, Georgia Institute of Technology, Atlanta, GA, USA, 2006.
20. Yeo, L.Y.; Kueh, P.G.; Choo, C.S.; Lee, S.H.; Zhang, D. Feature Visualization Using a Deep Learning Technique with Attention-Based Mechanism for Pipe Jacking through "Soft Rocks". In *Proceedings of the Geo-Risk 2023*; American Society of Civil Engineers: Reston, VA, USA, 2023; pp. 42–54.
21. Phangkawira, F. Charecterisation of Highly Weathered Phyllite via In-Situ Pressuremeter Test for the Assessment of Pipe-Jacking Forces. Ph.D. Thesis, Swinburne University of Technology Sarawak Campus, Kuching, Malaysia, 2019.
22. Peerun, M.I.; Ong, D.E.L.; Choo, C.S.; Cheng, W.C. Effect of Interparticle Behavior on the Development of Soil Arching in Soil-Structure Interaction. *Tunn. Undergr. Space Technol.* **2020**, *106*, 103610. [CrossRef]
23. Jong, S.C.; Ong, D.E.L.; Oh, E. State-of-the-Art Review of Geotechnical-Driven Artificial Intelligence Techniques in Underground Soil-Structure Interaction. *Tunn. Undergr. Space Technol.* **2021**, *113*, 103946. [CrossRef]
24. Wang, H.; He, M. Determining Method of Tensile Strength of Rock Based on Friction Characteristics in the Drilling Process. *Rock Mech. Rock Eng.* **2023**, *56*, 4211–4227. [CrossRef]
25. Osumi, T. Calculating Jacking Forces for Pipe Jacking Methods. *No-Dig Int. Res.* **2000**, *1*, 40–42.
26. Cheng, W.C.; Bai, X.D.; Sheil, B.B.; Li, G.; Wang, F. Identifying Characteristics of Pipejacking Parameters to Assess Geological Conditions Using Optimisation Algorithm-Based Support Vector Machines. *Tunn. Undergr. Space Technol.* **2020**, *106*, 103592. [CrossRef]
27. Erharter, G.H.; Marcher, T.; Reinhold, C. Application of Artificial Neural Networks for Underground Construction–Chances and Challenges–Insights from the BBT Exploratory Tunnel Ahrental Pfons. *Geomech. Und Tunnelbau* **2019**, *12*, 472–477. [CrossRef]
28. Fu, X.; Wu, M.; Tiong, R.L.K.; Zhang, L. Data-Driven Real-Time Advanced Geological Prediction in Tunnel Construction Using a Hybrid Deep Learning Approach. *Autom. Constr.* **2023**, *146*, 104672. [CrossRef]
29. Xu, D.; Wang, Y.; Huang, J.; Liu, S.; Xu, S.; Zhou, K. Prediction of Geology Condition for Slurry Pressure Balanced Shield Tunnel with Super-Large Diameter by Machine Learning Algorithms. *Tunn. Undergr. Space Technol.* **2023**, *131*, 104852. [CrossRef]
30. Zhang, N.; Zhou, A.; Pan, Y.; Shen, S.L. Measurement and Prediction of Tunnelling-Induced Ground Settlement in Karst Region by Using Expanding Deep Learning Method. *Measurement* **2021**, *183*, 109700. [CrossRef]
31. He, S.Y.; Tang, C.; Zhou, W.H. Settlement Prediction of Immersed Tunnel Considering Time-Dependent Foundation Modulus. *Tunn. Undergr. Space Technol.* **2024**, *144*, 105562. [CrossRef]
32. Wang, G.; Fang, Q.; Du, J.; Wang, J.; Li, Q. Deep Learning-Based Prediction of Steady Surface Settlement Due to Shield Tunnelling. *Autom Constr* **2023**, *154*, 105006. [CrossRef]
33. Shiau, J.; Sams, M.; Arvin, M.R.; Jongpradist, P. Automating the Process for Estimating Tunneling Induced Ground Stability and Settlement. *Geosciences* **2023**, *13*, 81. [CrossRef]
34. Nie, C.; Zhang, D.; Ouyang, L.; Huang, X.; Zhang, B.; Tong, Y. Dynamic Prediction of Longitudinal Settlement of Existing Tunnel Using ConvRes-DLinear Model with Integration of Undercrossing Construction Process Information. *Geosciences* **2023**, *13*, 189. [CrossRef]
35. Liu, L.; Zhou, W.; Gutierrez, M. Physics-Informed Ensemble Machine Learning Framework for Improved Prediction of Tunneling-Induced Short- and Long-Term Ground Settlement. *Sustainability* **2023**, *15*, 11074. [CrossRef]
36. Chen, H.; Xiao, C.; Yao, Z.; Jiang, H.; Zhang, T.; Guan, Y. Prediction of TBM Tunneling Parameters through an LSTM Neural Network. In Proceedings of the IEEE International Conference on Robotics and Biomimetics, Dali, China, 6–8 December 2019; IEEE: Dali, China, 2019.

37. Gao, M.Y.; Zhang, N.; Shen, S.L.; Zhou, A. Real-Time Dynamic Earth-Pressure Regulation Model for Shield Tunneling by Integrating GRU Deep Learning Method with GA Optimization. *IEEE Access* **2020**, *8*, 64310–64323. [CrossRef]
38. Nagrecha, K.; Fisher, L.; Mooney, M.; Rodriguez-Nikl, T.; Mazari, M.; Pourhomayoun, M. As-Encountered Prediction of Tunnel Boring Machine Performance Parameters Using Recurrent Neural Networks. *Transp. Res. Rec.* **2020**, *2674*, 241–249. [CrossRef]
39. Wei, X.J.; Wang, X.; Wei, G.; Zhu, C.W.; Shi, Y. Prediction of Jacking Force in Vertical Tunneling Projects Based on Neuro-Genetic Models. *J. Mar. Sci. Eng.* **2021**, *9*, 71. [CrossRef]
40. Flor, A.; Sassi, F.; La Morgia, M.; Cernera, F.; Amadini, F.; Mei, A.; Danzi, A. Artificial Intelligence for Tunnel Boring Machine Penetration Rate Prediction. *Tunn. Undergr. Space Technol.* **2023**, *140*, 105249. [CrossRef]
41. Briaud, J.-L. *The Pressuremeter*; Routledge: London, UK, 2019; ISBN 9780203736173.
42. Clarke, B.G. *Pressuremeters in Geotechnical Design*; CRC Press: London, UK, 2022; ISBN 9781003028925.
43. Yu, H.-S. *Cavity Expansion Methods in Geomechanics*; Springer Science + Business Media, LLC: Berlin/Heidelberg, Germany, 2000; ISBN 978-90-481-4023-7.
44. Ong, D.E.L.; Barla, M.; Cheng, J.W.C.; Choo, C.S.; Sun, M.; Peerun, M.I. *Sustainable Pipe-Jacking Technology in Urban Environment–Recent Advances and Innovations*; Springer Nature Singapore Pte Ltd.: Singapore, 2022; ISBN 978-981-16-9372-4.
45. Yu, H.S.; Houlsby, G.T. Finite Cavity Expansion in Dilatant Soils: Loading Analysis. *Géotechnique* **1991**, *41*, 173–183. [CrossRef]
46. Jin, Y.; Gardoni, P.; Biscontin, G. A Bayesian Definition of "most Probable" Parameters. *Geotech. Res.* **2018**, *5*, 130–142. [CrossRef]
47. Dai, Z.; Li, P.; Liu, J.; Liu, X.; Rui, Y.; Zhai, Y. Data-Driven Prediction for Curved Pipe Jacking Performance during Underwater Excavation of Ancient Shipwreck Using an Attention-Based Graph Convolutional Network Approach. *Expert Syst. Appl.* **2024**, *236*, 121393. [CrossRef]
48. Xu, K.; Ba, J.; Kiros, R.; Cho, K.; Courville, A.; Salakhutdinov, R.; Zemel, R.; Bengio, Y. Show, Attend and Tell: Neural Image Caption Generation with Visual Attention. In Proceedings of the Proceedings of the 32nd International Conference on Machine Learning; Bach, F., Blei, D., Eds.; PMLR: Lille, France, 2015; Volume 37, pp. 2048–2057.
49. Luong, M.-T.; Pham, H.; Manning, C.D. *Effective Approaches to Attention-Based Neural Machine Translation*; Association for Computational Linguistics: Lisbon, Portugal, 2015.
50. Sermanet, P.; Kavukcuoglu, K.; Chintala, S.; Lecun, Y. Pedestrian Detection with Unsupervised Multi-Stage Feature Learning. In Proceedings of the IEEE Computer Society Conference on Computer Vision and Pattern Recognition, Portland, OR, USA, 23–28 June 2013; pp. 3626–3633.
51. Duro, D.C.; Franklin, S.E.; Dubé, M.G. A Comparison of Pixel-Based and Object-Based Image Analysis with Selected Machine Learning Algorithms for the Classification of Agricultural Landscapes Using SPOT-5 HRG Imagery. *Remote Sens. Environ.* **2012**, *118*, 259–272. [CrossRef]
52. Yang, C.; Hassani, F.; Zhou, K.; Zhang, Q.; Wang, F.; Gao, F.; Topa, A. Numerical Investigation of TBM Disc Cutter Cutting on Microwave-Treated Basalt with an Unrelieved Model. *Arch. Civ. Mech. Eng.* **2022**, *22*, 147. [CrossRef]
53. Cheng, J.-L.; Wang, Y.-X.; Wang, L.-G.; Li, Y.-H.; Hu, B.; Jiang, Z.-H. Penetration Behaviour of TBM Disc Cutter Assisted by Vertical Precutting Free Surfaces at Various Depths and Confining Pressures. *Arch. Civ. Mech. Eng.* **2021**, *21*, 22. [CrossRef]
54. Chen, X.-J.; Fu, Y.; Liu, Y. Random Finite Element Analysis on Uplift Bearing Capacity and Failure Mechanisms of Square Plate Anchors in Spatially Variable Clay. *Eng. Geol.* **2022**, *304*, 106677. [CrossRef]
55. Kang, Q.; Chen, E.J.; Li, Z.-C.; Luo, H.-B.; Liu, Y. Attention-Based LSTM Predictive Model for the Attitude and Position of Shield Machine in Tunneling. *Undergr. Space* **2023**, *13*, 335–350. [CrossRef]
56. Liu, Z.; Li, L.; Fang, X.; Qi, W.; Shen, J.; Zhou, H.; Zhang, Y. Hard-Rock Tunnel Lithology Prediction with TBM Construction Big Data Using a Global-Attention-Mechanism-Based LSTM Network. *Autom. Constr.* **2021**, *125*, 103647. [CrossRef]
57. Gao, Y.; Chen, R.; Qin, W.; Wei, L.; Zhou, C. Learning from Explainable Data-Driven Tunneling Graphs: A Spatio-Temporal Graph Convolutional Network for Clogging Detection. *Autom. Constr.* **2023**, *147*, 104741. [CrossRef]
58. Choo, C.S.; Ong, D.E.L.; Phangkawira, F.; Yeo, L.Y.; Lee, S.H. Evaluation of Jacking Forces in Weathered Phyllite: Geomaterial Characterization and Deep Learning Techniques. In Proceedings of the International No-Dig 2022, 38th International Conference and Exhibition, Helsinki, Finland, 3–5 October 2022.
59. Yeo, L.Y.; Choo, C.S.; Lee, S.H. To Jack or Not to Jack: Inside the Minds of Pipe Jacking Operators. In *Proceedings of ASEAN-Australian Engineering Congress*; Springer Nature Singapore Pte Ltd.: Singapore, 2023.
60. Mourchid, Y.; Slama, R. D-STGCNT: A Dense Spatio-Temporal Graph Conv-GRU Network Based on Transformer for Assessment of Patient Physical Rehabilitation. *Comput. Biol. Med.* **2023**, *165*, 107420. [CrossRef] [PubMed]
61. Zhang, H.; Feng, L.; Wang, J.; Gao, N. Development of Technology Predicting Based on EEMD-GRU: An Empirical Study of Aircraft Assembly Technology. *Expert Syst. Appl.* **2024**, *246*, 123208. [CrossRef]
62. *ASTM D4719-07*; Standard Test Methods for Prebored Pressuremeter Testing in Soils. ASTM: West Conshohocken, PA, USA, 2020.
63. Stein, D. *Practical Guideline for the Application of Microtunnelling Methods for the Ecological, Cost-Minimised Installation of Drains and Sewers*; Stein und Partner: Bochum, Germany, 2005.

64. Ates, U.; Bilgin, N.; Copur, H. Estimating Torque, Thrust and Other Design Parameters of Different Type TBMs with Some Criticism to TBMs Used in Turkish Tunneling Projects. *Tunn. Undergr. Space Technol.* **2014**, *40*, 46–63. [CrossRef]
65. Choo, C.S.; Ong, D.E.L. Determination of Jacking Forces Based on Highly Weathered Non-Linear "soft Rock" Strength Parameters Considering Arching. In Proceedings of the 16th Asian Regional Conference on Soil Mechanics and Geotechnical Engineering, Taipei, Taiwan, 4–18 October 2019.